Noncanonical contributions of MutLγ to VDE-initiated crossovers during *Saccharomyces cerevisiae* meiosis

Anura Shodhan[1], Darpan Medhi[1,2], and Michael Lichten[1]*

[1] Laboratory of Biochemistry and Molecular Biology, Center for Cancer Research, National Cancer Institute, Bethesda, Maryland, USA
[2] Current address: Developmental Biology Program, Sloan Kettering Institute, Memorial Sloan Kettering Cancer Center, New York, USA
* Correspondence: michael.lichten@nih.gov

In *Saccharomyces cerevisiae*, the meiosis-specific axis proteins Hop1 and Red1 are present nonuniformly across the genome. In a previous study, the meiosis-specific *VMA1*-derived endonuclease (VDE) was used to examine Spo11-independent recombination in a recombination reporter inserted in a Hop1/Red1-enriched region (*HIS4*) and in a Hop1/Red1-poor region (*URA3*). VDE-initiated crossovers at *HIS*4 were mostly dependent on Mlh3, a component of the MutLγ meiotic recombination intermediate resolvase, while VDE-initiated crossovers at *URA3* were mostly Mlh3-independent. These differences were abolished in the absence of the chromosome axis remodeler Pch2, and crossovers at both loci become partly Mlh3-dependent. To test the generality of these observations, we examined inserts at six additional loci that differed in terms of Hop1/Red1 enrichment, chromosome size, and distance from centromeres and telomeres. All six loci behaved similarly to *URA3*: the vast majority of VDE-initiated crossovers were Mlh3-independent. This indicates that, counter to previous suggestions, meiotic chromosome axis protein enrichment is not a primary determinant of which recombination pathway gives rise to crossovers during VDE-initiated meiotic recombination. In *pch2*Δ mutants, the fraction of VDE-induced crossovers that were Mlh3-dependent increased to levels previously observed for Spo11-initiated crossovers in *pch2*Δ, indicating that Pch2-dependent processes play an important role in controlling the distribution of factors necessary for MutLγ-dependent crossovers.

Introduction

During meiosis, the crossover products of recombination form stable links between homologous chromosomes of different parental origin (homologs), to enable their proper segregation during the meiotic divisions (reviewed by Zickler and Kleckner 1999; Whitby 2005). Meiotic recombination is initiated by DNA double strand breaks (DSBs) that are formed by the meiosis-specific Spo11 protein (Bergerat *et al.* 1997; Keeney 2001). In budding yeast, Spo11 DSBs are unevenly distributed in the genome. Most DSB-rich regions correlate with domains that are enriched for the meiosis-specific chromosome axis proteins, Red1 and Hop1, which play an important role in DSB formation (Hollingsworth and Ponte 1997; Blat *et al.* 2002; Pan *et al.* 2011; Panizza *et al.* 2011; Smagulova *et al.* 2011; Baker *et al.* 2014). The non-uniform distribution of Hop1 is maintained by Pch2, a hexameric AAA+ ATPase (Chen *et al.* 2014). In *pch2* mutants, Hop1 persists longer and is more uniformly distributed on chromosomes; this is accompanied by a delay in meiotic progression and changes in the distribution of late-forming DSBs and COs (Börner *et al.* 2008; Joshi *et al.* 2009; Zanders and Alani 2009; Lambing *et al.* 2015; Subramanian *et al.* 2016; Subramanian *et al.* 2018).

Meiotic DSBs are also important for homolog colocalization, pairing and synapsis (Keeney *et al.* 1997; Romanienko and Camerini-Otero 2000; Baudat *et al.* 2013). Current thinking is that most DSBs are repaired either by a synthesis-dependent strand annealing pathway that forms non-crossovers (NCOs), or by a pathway that forms double Holiday junction (dHJ) intermediates that are resolved as crossovers (COs) by the MutLγ (Mlh1-Mlh3 and Exo1) meiosis-specific resolvase (Schwacha and Kleckner 1994; Wang *et al.* 1999; Khazanehdari and Borts 2000; Kirkpatrick *et al.* 2000; Tsubouchi and Ogawa 2000; Allers and Lichten 2001b; Allers and Lichten 2001a; Hoffmann *et al.* 2003; Argueso *et al.* 2004; Bishop and Zickler 2004; Nishant *et al.* 2008; Zakharyevich *et al.* 2010; Al-Sweel *et al.* 2017). In budding yeast, COs and NCOs are formed at similar levels, suggesting that roughly equal fractions of DSBs are repaired by these two pathways (Martini *et al.* 2006; Mancera *et al.* 2008). Apart from these two major pathways, a minor pathway uses mitotic resolvases (structure-selective nucleases, SSNs: Mus81-Mms4, Yen1 and Slx1-4) to form both NCOs and COs (de los Santos *et al.* 2003; Argueso *et al.* 2004; Lynn *et al.* 2007; Jessop and Lichten 2008; De Muyt *et al.* 2012; Zakharyevich *et al.* 2012; Agostinho *et al.* 2013; Oke *et al.* 2014). While the proteins and enzymatic activities contributing to each of these pathways has been the subject of considerable study (reviewed by Ehmsen and Heyer 2008; Hunter 2015; Manhart and Alani 2016) , the question of what roles local chromosome environment might play in pathway choice remains much less explored. (Medhi *et al.* 2016) addressed this question using a meiosis-specific endonuclease, VDE, that cleaves a recognition sequence (VRS) at high efficiency regardless of chromosomal context (Gimble and Thorner 1992; Gimble and Thorner 1993; Nogami *et al.* 2002; Fukuda *et al.* 2003; Medhi *et al.* 2016; this work). Like Spo11 DSBs, VDE DSBs are processed to form single-stranded overhangs that recruit the Rad51 and Dmc1 proteins that perform strand invasion and homology search (Bishop *et al.* 1992; Fukuda *et al.* 2003; Fukuda and Ohya 2006). Medhi *et al.* (2016) inserted a VRS-containing recombination reporter at two loci: *HIS4*, present in a region with high levels of both Spo11 DSBs and Hop1 binding; and *URA3*, in a region with low levels of Spo11 DSBs and Hop1 binding (Pan *et al.* 2011; Panizza *et al.* 2011). Most COs at *HIS4* were Mlh3-dependent, while COs at *URA3* were Mlh3-independent. In *pch2*Δ mutants, Hop1 occupancy at *HIS4* was reduced, as were the fraction of COs that were Mlh3-dependent, while at *URA3* the fraction of COs that were Mlh3-dependent increased. Based on these findings, Medhi *et al.* suggested that the local chromosome structure, in particular levels of Hop1 enrichment, may be an important determinant of CO pathway choice.

To test the generality of the above suggestion, we inserted the same VRS recombination reporter at six new loci with varying Hop1 occupancy in their vicinity and found that VDE-initiated meiotic COs at all six new loci were predominantly Mlh3-independent. Moreover, as previously seen for inserts at *URA3* (Medhi *et al.* 2016), *pch2*Δ mutation increased the fraction of COs that were Mlh3-dependent. These results indicate that the local level of Hop1 enrichment is not the sole determinant of CO pathway choice in VDE-induced meiotic recombination. They also suggest that, at most loci, VDE DSBs are repaired differently than are Spo11 DSBs.

Materials and Methods

Yeast strains

All strains (Table S2) used in this study are of SK1 background (KANE AND ROTH 1974), and were constructed by transformation or genetic crosses. The recombination reporter cassette with the VRS (cleavable) or VRS-103 (uncleavable) site in the *ARG4* gene (MEDHI *et al.* 2016) were inserted by ends-out transformation (for VRS-containing inserts and for VRS-103 inserts at *FIR1* and *HSP30*, Figure S1A) or by ends-in transformation (for VRS-103 constructs at *CCT6*, *RIM15*, *IMD3* and *TRK2*, Figure S1B) at six different locations (primers used are listed in Table S1). Ends-in transformation was used for inserts at divergently transcribed loci to minimize effects on expression caused by disruption of 5' untranslated regions. Transformation was performed with overlapping DNA fragments as illustrated in Figure S1. The VRS-*arg4* and VRS-103-*arg4* constructs are 5.5kb and 8.6kb long, respectively, with ~3kb sequence homology around the VRS site. This size difference, along with *Hin*dIII site differences, enables the detection of the parental and recombinant chromosomes on Southern blots (see Figure 2, below).

Growth and sporulation

Strains were grown in pre-sporulation SPS medium and transferred to sporulation medium as described (GOYON AND LICHTEN 1993), with the inclusion of 10μM $CuSO_4$ in sporulation medium to induce VDE expression (MEDHI *et al.* 2016). DNA samples were collected and processed as described (ALLERS AND LICHTEN 2000; JESSOP *et al.* 2005; JESSOP *et al.* 2006).

DNA extraction and southern hybridization

DNA was extracted from samples using the CTAB extraction method (ALLERS AND LICHTEN 2000; OH *et al.* 2009). Genomic DNA was digested with *Hin*dIII or *Hin*dIII and PI-*Sce*I, run on agarose gels, blotted, probed and analyzed as described (MEDHI *et al.* 2016).

Cytology

Cells were collected, stained with DAPI, and scored by epifluoresence microscopy to follow nuclear divisions as described (KAUR *et al.* 2018).

Statistical analysis

GraphPad Prism was used for comparisons of mean values, using t-tests with the Holm-Sidak correction for multiple comparisons.

Data availability

Strains and plasmids are available upon request. The authors affirm that all data necessary for confirming the conclusions of this article are represented fully within the article, tables, figures, supplementary figures and supplementary tables. Underlying data for all graphs will be made available in Supplementary File 1 upon publication.

Results and Discussion

VDE-initiated COs are Mlh3-independent at most insert sites

To further test the hypothesis that Hop1-enrichment determines the MutLγ-dependence of meiotic CO formation, six new sites were selected for VRS reporter insertion, one (*HSP30*) with regional Hop1 levels similar to those at *URA3*, and five (*CCT6*, *FIR1*, *RIM15, TRK2* and *IMD3*) with regional Hop1 levels similar to those at *HIS4* (Figure 1). Since it has been previously shown that Spo11-DSBs are reduced near centromeres and telomeres (PAN *et al.* 2011) and CO formation is regulated differently on longer and shorter chromosomes (JOSHI *et al.* 2009; ZANDERS AND ALANI 2009), the new sites were selected such that they were on chromosomes of different sizes and were at varying distances from centromeres and telomeres. At each site, recombination products can be differentiated on Southern blots (Figure 2A, B), as was previously used to quantify DSBs, COs and NCOs (MEDHI *et al.* 2016).

Meiotic progression of all WT and *mlh3*Δ strains was similar, with most cells completing the first meiotic division by 7-8h post-induction (Figure S2A). In addition, VDE-initiated DSBs appeared and disappeared with levels and timing similar to those previously seen at

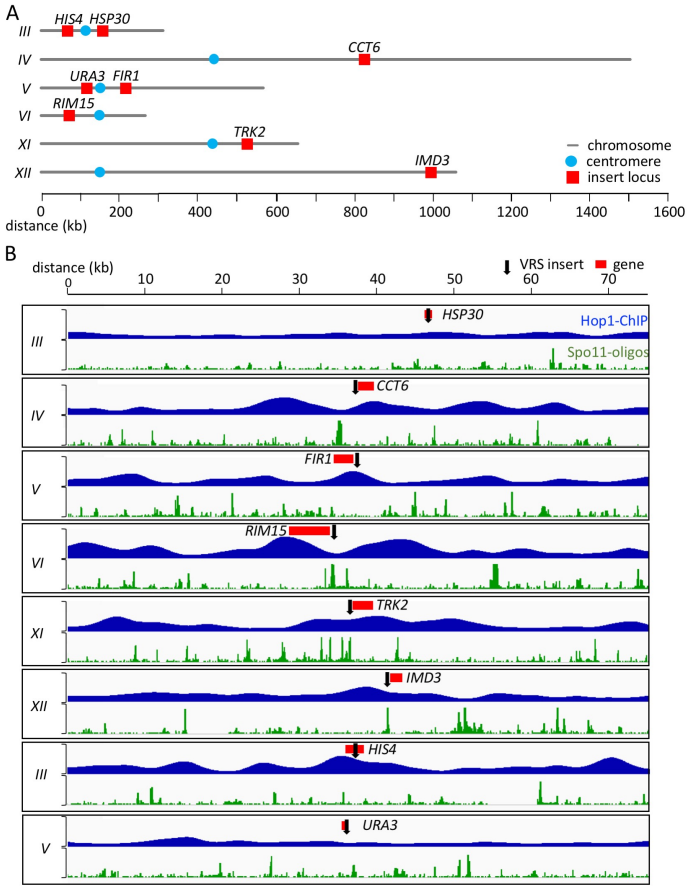

Figure 1. Insert loci examined. (A) Locations of insert loci are illustrated (red). Blue circles denote centromere locations. (B) Maps of regions surrounding insert loci. Red—coding region of gene used to identify each insert; black arrow—site of VRS insert. Blue plots show relative Hop1 occupancy levels in mid meiosis, using smoothed ChIP-chip data from (PANIZZA *et al.* 2011); vertical scale = 0-7, decile-normalized ChIP/WCE. Green plots show relative DSB levels, using Spo11-oligo reads from PAN *et al.* (2011); vertical scale = 0-15 hits per million/base-pair.

HIS4 and *URA3* (Figure S2B; MEDHI *et al.* 2016).

COs in VRS inserts ranged from ~6% of total lane signal at *CCT6* to ~10.3% at *HIS4* (Figure 2C). As previously reported (MEDHI *et al.* 2016), NCOs were recovered in substantial excess over COs at all insert loci (Figure 2E), with NCO/CO ratios ranging from 2.1 to 4.8 (mean = 3.1 ± 0.8; Figure S2C). The marked excess of NCOs over COs seen for VDE-initiated events differs from what is seen with Spo11-initiated events, where COs and NCOs are produced at similar levels (MARTINI *et al.* 2006; MANCERA *et al.* 2008; ZAKHARYEVICH *et al.* 2012). In contrast to what was seen for VRS inserts at *HIS4*, where COs were reduced dramatically in *mlh3*Δ mutants (to ~40% of wild-type levels), COs in the same sequences inserted at all other loci were only modestly affected, with COs in *mlh3*Δ ranging from ~80% to ~115% of wild type (mean = 91 ± 12%; Figure 2D); NCOs were similarly unaffected (Figure 2E, F). These results indicate that, in contrast to Spo11-initiated COs, which are reduced about 2-fold in *mlh3*Δ mutants (WANG *et al.* 1999; KHAZANEHDARI AND BORTS 2000; KIRKPATRICK *et al.* 2000; TSUBOUCHI AND OGAWA 2000; HOFFMANN *et al.* 2003; ARGUESO *et al.*

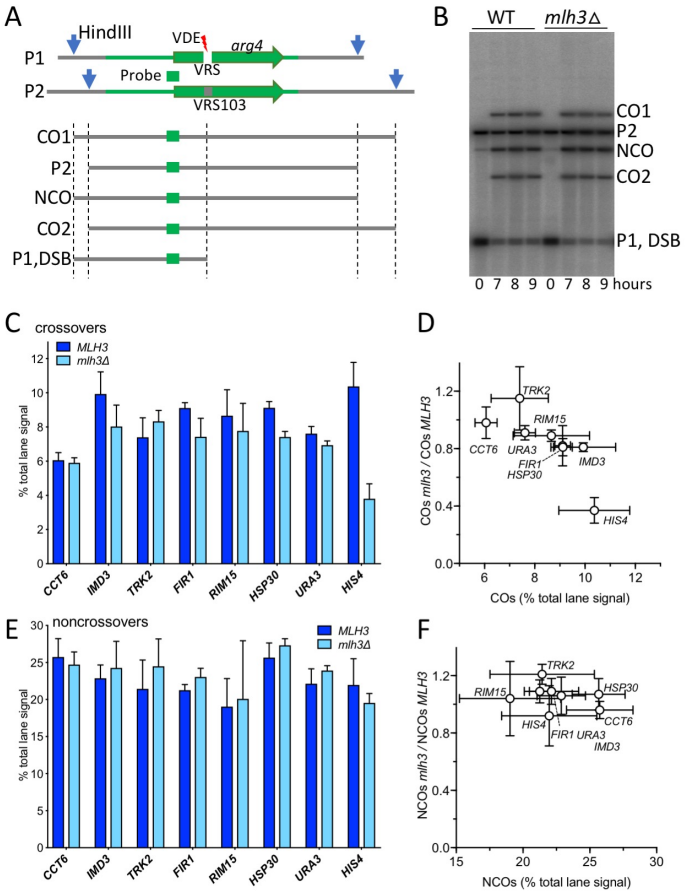

Figure 2. VDE-initiated crossovers at most loci are MutLγ-independent. (A) Strategy for detection of VDE-initiated COs and NCOs. A cartoon of the VRS and VRS-103 inserts is shown, illustrating : white box—VRS sequences; blue arrows—*Hin*dIII restriction sites; green lines—sequences shared between the two inserts, with *ARG4* coding sequences shown as a green arrow; green box—sequences used for Southern blot probes. Digestion with *Hin*dIII and PI-*Sce*I (VDE) distinguishes parental (P1 and P2), CO and NCO products. VDE-cut inserts are not distinguished from parent P1 on these digests, but can be distinguished in digests with *Hin*dIII alone (MEDHI *et al.* 2016). (B) Representative Southern blot containing DNA from strains with inserts at *RIM15*. (C) VDE-initiated COs in *MLH3* and *mlh3*Δ cells. CO frequencies, average signal of CO1 and CO2 for 8 and 9 h samples from three independent experiments for inserts at *HIS4* and from two independent experiments for inserts at all other loci. Data for inserts at *URA3* and for two experiments with inserts at *HIS4* are from MEDHI *et al.,* (2016). (D) fraction of COs that are MutLγ-independent (ratio of CO frequencies in *mlh3*Δ versus *MLH3*), plotted as a function of CO frequencies in *MLH3* strains. CO frequencies in *MLH3* and *mlh3*Δ differ significantly only for inserts at *HSP30* and *HIS4* (adjusted *p* values of 0.003 and 0.0001, respectively) (E,F) VDE-initiated NCOs, details as in (B) and (C); frequencies in *MLH3* and *mlh3*Δ do not differ significantly at any locus. Error bars in all panels denote standard deviation.

2004; NISHANT *et al.* 2008; AL-SWEEL *et al.* 2017; CHAKRABORTY *et al.* 2017), most COs at the VDE break sites are formed independent of MutLγ, irrespective of the chromosome size, distance from centromere or telomere, or Hop1-enrichment in their vicinity. Thus, at most insert loci in otherwise wild-type cells, VDE-initiated recombination differs from Spo11-initiated recombination and more closely resembles mitotic recombination, in that NCOs are in excess over COs (ESPOSITO 1978; LICHTEN AND HABER 1989; IRA *et al.* 2003; DAYANI *et al.* 2011) and, with the exception of those formed in inserts at *HIS4*, VDE-initiated COs are largely MutLγ-independent.

Increased Mlh3-dependence of VDE-initiated COs in pch2Δ *mutants*

In *pch2* mutants, meiotic axis proteins are redistributed, with less pronounced differences in Hop1 occupancy distributions measured either cytologically (BÖRNER *et al.* 2008; JOSHI *et al.* 2009) or by chromatin-immunoprecipitation (MEDHI *et al.* 2016). Previously, we found that the absence of Pch2 did not substantially alter overall NCO or CO levels at *HIS4* and *URA3,* but the Mlh3-dependence of CO formation was affected at both loci, with Mlh3-independent COs increasing at *HIS4* and decreasing at *URA3*. Because the six new VRS insert loci studied here are similar to *URA3*, in that most VDE-initiated COs are Mlh3-independent, we wanted to see if COs at these loci also displayed increased Mlh3-dependence in *pch2*Δ mutants.

Consistent with previous findings (BÖRNER *et al.* 2008), meiotic divisions were delayed in *pch2*Δ and *pch2*Δ *mlh3*Δ mutants relative to wild type (Figure S2A). Frequencies of NCOs at all eight VRS insert loci in the *pch2*Δ were similar to those seen in wild type (Figure 3C; *pch2*Δ/*PCH2* = 111 ± 10%), as were COs (Figure 3A; *pch2*Δ/*PCH2* = 113 ± 16%). Loss of Mlh3 did not substantially affect NCOs in the absence of Pch2 (Figure 3C; *pch2*Δ *mlh3*Δ/*pch2*Δ *MLH3* = 114 ± 14%). However, in *pch2*Δ *mlh3*Δ double mutants, COs were reduced 20-35% relative to *pch2*Δ *MLH3* (Figure 3B; average *pch2*Δ *mlh3*Δ/*pch2*Δ = 74 ± 7%), as was previously observed for inserts at *URA3* and *HIS4* (MEDHI *et al.* 2016). A quantitatively similar MutLγ-dependence has also been observed for Spo11-initiated COs in *pch2*Δ mutants, both genome-wide (*pch2*Δ *mlh3*Δ / *pch2*Δ = 73% (CHAKRABORTY *et al.* 2017) and for individual genetic intervals (*pch2*Δ / *pch2*Δ *mlh3*Δ = 75%, calculated from combined data of NISHANT *et al.* 2008; ZANDERS AND ALANI 2009; AL-SWEEL *et al.* 2017; CHAKRABORTY *et al.* 2017). Thus, the absence of Pch2 increases the MutLγ-dependence of VDE-initiated COs at many loci, while decreasing the MutLγ-dependence of VDE-initiated COs at *HIS4* and of Spo11-initiated COs.

Spo11-initiated COs are reduced about 2-fold in mutants lacking MutLγ; this is thought to reflect unbiased JM resolution by SSNs to form both COs and NCOs, as opposed to MutLγ-mediated biased JM resolution as COs in wild type (ARGUESO *et al.* 2004; ZAKHARYEVICH *et al.* 2012). If the same holds true for *pch2* mutants, the ~25% reduction in COs seen in *pch2*Δ *mlh3*Δ would suggest that about half of the COs formed in *pch2 MLH3* cells are the products of MutLγ-mediated resolution, regardless of whether they were initiated by VDE or by Spo11. It therefore appears that Pch2, or factors regulated by it, prevents most VDE-initiated events from forming MutLγ-dependent COs.

Summary and concluding remarks

In this study, we examined VDE-initiated meiotic recombination in a recombination reporter inserted at six loci in addition to the two loci (*HIS4* and *URA3*) originally examined by MEDHI *et al.* (2016). With the exception of *HIS4*, VDE-initiated COs at all insert loci were largely Mlh3-independent, regardless of whether inserts were at loci in Hop1-enriched or Hop1-depleted regions of the genome. Therefore, the hypothesis proposed by MEDHI *et al.*, that local Hop1 occupancy determines mechanisms of JM resolution, is incorrect, at least for VDE-initiated recombination, in that it was based on analysis of inserts at a locus (*HIS4*) that appears to be exceptional.

The observation that VDE-initiated COs at most insert loci are Mlh3-independent, in turn, raises the question of whether or not VDE-initiated recombination events that occur in cells undergoing meiosis can be properly described as being “meiotic”. VDE-initiated NCOs are

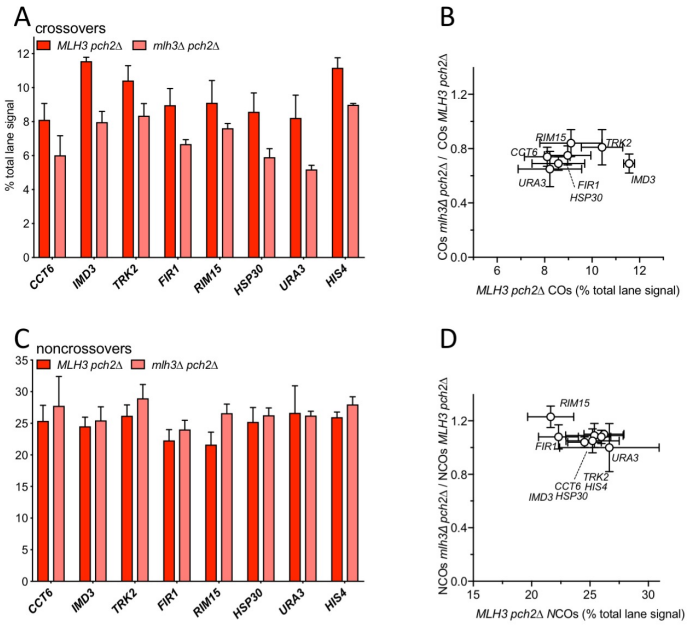

Figure 3. VDE-initiated crossovers in *pch2*Δ mutants are partially MutLγ-dependent. (A) VDE-initiated COs in *MLH3 pch2*Δ and *mlh3*Δ *pch2*Δ cells. (A) CO frequencies, average signal of CO1 and CO2 for 8 and 9 h samples from two independent experiments. For inserts at *CCT6*, *IMD3*, *FIR1* and *RIM15*, 9 h values are from a single experiment. Data for inserts at *HIS4* and *URA3* are from MEDHI *et al.* (2016). (B) fraction of COs that are MutLγ-independent (ratio of CO frequencies in *mlh3*Δ versus *MLH3*), plotted as a function of CO frequencies in *MLH3* strains. CO frequencies in *MLH3 pch2*Δ and *mlh3*Δ *pch2*Δ differ significantly for inserts at all loci (adjusted *p* values ≤ 0.03) except *CCT6* and *RIM15* (adjusted *p* values of 0.06 and 0.07, respectively). (C, D) VDE-initiated NCOs, as in panels (A) and (B). NCO frequencies in *MLH3 pch2*Δ and *mlh3*Δ *pch2*Δ do not differ significantly for any locus. Error bars in all panels denote standard deviation.

recovered in excess of COs (2 to 5-fold, average 3.2 ± 0.1), which is reminiscent of, although less than, the 5 to 20-fold excess of NCOs over COs seen in budding yeast mitotic recombination (ESPOSITO 1978; LICHTEN AND HABER 1989; IRA *et al.* 2003; BZYMEK *et al.* 2010; DAYANI *et al.* 2011). VDE-initiated DSB processing also resembles DSB processing in the mitotic cell cycle, in that break ends are continuously resected over time (LEE *et al.* 1998; NEALE *et al.* 2002; JOHNSON *et al.* 2007), unlike the limited resection seen with Spo11 DSBs (MIMITOU *et al.* 2017). Finally, unlike Spo11, VDE frequently cuts both sister chromatids in a single meiosis (GIMBLE AND THORNER 1992; GIMBLE AND THORNER 1993; MEDHI *et al.* 2016), and gene CO/NCO ratio among HO endonuclease-initiated meiotic recombinants (MALKOVA *et al.* 2000). Further studies will be necessary to determine which of these or other factors are responsible for the marked Mlh3-independence of VDE-initiated COs at seven of the eight insert locations examined, and why the majority of VDE-initiated COs at *HIS4* are Mlh3-dependent.

In contrast, in *pch2*Δ strains, VDE-initiated COs show the same Mlh3-dependence as Spo11-initiated COs, regardless of wild-type Hop1 occupancy levels at insert loci. It therefore seems unlikely that Hop1 redistribution in *pch2*Δ mutants is the only factor responsible for the increased Mlh3-dependence of COs at most insert loci and decreased Mlh3-dependence of COs at *HIS4*. Homolog synapsis, recombinant formation and meiotic divisions are all delayed in *pch2*Δ mutants, which also display a more even distribution of the Zip1 central element protein along chromosomes and reduced CO interference (BÖRNER *et al.* 2008; JOSHI *et al.* 2009; ZANDERS AND ALANI 2009). It is possible that, in *pch2*Δ mutants, these or other defects delay the recruitment of factors necessary for MutLγ-resolution at Spo11-initiated events, and thus make them available to VDE-initiated events. Again, further studies will be necessary to test these possibilities.

In summary, the data presented here indicate that VDE-initiated recombination events are treated differently than are those initiated by Spo11 during wild-type meiosis. VDE-initiated events produce an excess of NCOs over COs and, at seven of eight loci examined, form COs by MutLγ-independent mechanisms, and thus their outcome more closely resembles those of DSB repair events that occur during the mitotic cell cycle. We conclude that the full spectrum of meiotic recombination processes that occur at Spo11-initiated DSBs do not occur at VDE-initiated DSBs, and, by inference, DSBs formed during meiosis by other nucleases. Thus, our findings call for caution in the use of DSBs formed by these nucleases, or by other exogenous means, for inferring factors that control normal meiotic recombination.

End Matter

Author Contributions and Notes

A. S. and D. M. performed research, A. S., D. M. and M.L designed research, analyzed data and wrote the paper. The authors declare no conflict of interest.

Acknowledgments

We thank Jean Paul Ouyan, Seyoun Kim, and Matan Cohen for help in strain construction, and Jasvinder Ahuja, Matan Cohen, Julia Cooper, and Martin Xaver for comments and discussion. This work was supported by the Intramural Research Program of the NIH through the Center for Cancer Research at the National Cancer Institute.

References

Agostinho, A., B. Meier, R. Sonneville, M. Jagut, A. Woglar *et al.*, 2013 Combinatorial regulation of meiotic Holliday junction resolution in *C. elegans* by HIM-6 (BLM) helicase, SLX-4, and the SLX-1, MUS-81 and XPF-1 nucleases. PLoS Genet 9**:** e1003591.

Al-Sweel, N., V. Raghavan, A. Dutta, V. P. Ajith, L. Di Vietro *et al.*, 2017 *mlh3* mutations in baker's yeast alter meiotic recombination outcomes by increasing noncrossover events genome-wide. PLoS Genet 13**:** e1006974.

Allers, T., and M. Lichten, 2000 A method for preparing genomic DNA that restrains branch migration of Holliday junctions. Nucleic Acids Research 28**:** e6.

Allers, T., and M. Lichten, 2001a Differential timing and control of noncrossover and crossover recombination during meiosis. Cell 106**:** 47-57.

Allers, T., and M. Lichten, 2001b Intermediates of yeast meiotic recombination contain heteroduplex DNA. Mol Cell 8**:** 225-231.

Argueso, J. L., J. Wanat, Z. Gemici and E. Alani, 2004 Competing crossover pathways act during meiosis in *Saccharomyces cerevisiae*. Genetics 168**:** 1805-1816.

Baker, C. L., M. Walker, S. Kajita, P. M. Petkov and K. Paigen, 2014 PRDM9 binding organizes hotspot nucleosomes and limits Holliday junction migration. Genome Res 24**:** 724-732.

Baudat, F., Y. Imai and B. de Massy, 2013 Meiotic recombination in mammals: localization and regulation. Nat Rev Genet 14**:** 794-806.

Bergerat, A., B. de Massy, D. Gadelle, P. C. Varoutas, A. Nicolas *et al.*, 1997 An atypical topoisomerase II from Archaea with implications for meiotic recombination. Nature 386**:** 414-417.

Bishop, D. K., D. Park, L. Xu and N. Kleckner, 1992 *DMC1*: a meiosis-specific yeast homolog of E. coli *recA* required for recombination, synaptonemal complex formation, and cell cycle progression. Cell 69**:** 439-456.

Bishop, D. K., and D. Zickler, 2004 Early decision; meiotic crossover interference prior to stable strand exchange and synapsis. Cell 117**:** 9-15.

Blat, Y., R. U. Protacio, N. Hunter and N. Kleckner, 2002 Physical and functional interactions among basic chromosome organizational features govern early steps of meiotic chiasma formation. Cell 111**:** 791-802.

Börner, G. V., A. Barot and N. Kleckner, 2008 Yeast Pch2 promotes domainal axis organization, timely recombination progression, and arrest of defective recombinosomes during meiosis. Proc Natl Acad Sci U S A 105**:** 3327-3332.

Bzymek, M., N. H. Thayer, S. D. Oh, N. Kleckner and N. Hunter, 2010 Double Holliday junctions are intermediates of DNA break repair. Nature 464**:** 937-941.

Chakraborty, P., A. V. Pankajam, G. Lin, A. Dutta, G. N. Krishnaprasad *et al.*, 2017 Modulating crossover frequency and interference for obligate crossovers in *Saccharomyces cerevisiae* meiosis. G3 (Bethesda) 7**:** 1511-1524.

Chen, C., A. Jomaa, J. Ortega and E. E. Alani, 2014 Pch2 is a hexameric ring ATPase that remodels the chromosome axis protein Hop1. Proc Natl Acad Sci U S A 111**:** E44-53.

Dayani, Y., G. Simchen and M. Lichten, 2011 Meiotic recombination intermediates are resolved with minimal crossover formation during return-to-growth, an analogue of the mitotic cell cycle. PLoS Genet 7**:** e1002083.

de los Santos, T., N. Hunter, C. Lee, B. Larkin, J. Loidl *et al.*, 2003 The Mus81/Mms4 endonuclease acts independently of double-Holliday junction resolution to promote a distinct subset of crossovers during meiosis in budding yeast. Genetics 164**:** 81-94.

De Muyt, A., L. Jessop, E. Kolar, A. Sourirajan, J. Chen *et al.*, 2012 BLM helicase ortholog Sgs1 is a central regulator of meiotic recombination intermediate metabolism. Mol Cell 46**:** 43-53.

Ehmsen, K. T., and W. D. Heyer, 2008 Biochemistry of meiotic recombination: formation, processing, and resolution of recombination intermediates. Genome Dyn Stab 3**:** 91.

Esposito, M. S., 1978 Evidence that spontaneous mitotic recombination occurs at the two-strand stage. Proc Natl Acad Sci U S A 75**:** 4436-4440.

Fukuda, T., S. Nogami and Y. Ohya, 2003 VDE-initiated intein homing in *Saccharomyces cerevisiae* proceeds in a meiotic recombination-like manner. Genes Cells 8**:** 587-602.

Fukuda, T., and Y. Ohya, 2006 Recruitment of RecA homologs Dmc1p and Rad51p to the double-strand break repair site initiated by meiosis-specific endonuclease VDE (PI-SceI). Mol Genet Genomics 275**:** 204-214.

Gimble, F. S., and J. Thorner, 1992 Homing of a DNA endonuclease gene by meiotic gene conversion in *Saccharomyces cerevisiae*. Nature 357**:** 301-306.

Gimble, F. S., and J. Thorner, 1993 Purification and characterization of VDE, a site-specific endonuclease from the yeast *Saccharomyces cerevisiae*. J Biol Chem 268**:** 21844-21853.

Goyon, C., and M. Lichten, 1993 Timing of molecular events in meiosis in *Saccharomyces cerevisiae*: stable heteroduplex DNA is formed late in meiotic prophase. Mol Cell Biol 13**:** 373-382.

Hoffmann, E. R., P. V. Shcherbakova, T. A. Kunkel and R. H. Borts, 2003 *MLH1* mutations differentially affect meiotic functions in *Saccharomyces cerevisiae*. Genetics 163**:** 515-526.

Hollingsworth, N. M., and L. Ponte, 1997 Genetic interactions between *HOP1*, *RED1* and *MEK1* suggest that *MEK1* regulates assembly of axial element components during meiosis in the yeast *Saccharomyces cerevisiae*. Genetics 147**:** 33-42.

Hunter, N., 2015 Meiotic recombination: the essence of heredity. Cold Spring Harb Perspect Biol 7.

Ira, G., A. Malkova, G. Liberi, M. Foiani and J. E. Haber, 2003 Srs2 and Sgs1-Top3 suppress crossovers during double-strand break repair in yeast. Cell 115**:** 401-411.

Jessop, L., T. Allers and M. Lichten, 2005 Infrequent co-conversion of markers flanking a meiotic recombination initiation site in *Saccharomyces cerevisiae*. Genetics 169**:** 1353-1367.

Jessop, L., and M. Lichten, 2008 Mus81/Mms4 endonuclease and Sgs1 helicase collaborate to ensure proper recombination intermediate metabolism during meiosis. Mol Cell 31**:** 313-323.

Jessop, L., B. Rockmill, G. S. Roeder and M. Lichten, 2006 Meiotic chromosome synapsis-promoting proteins antagonize the anti-crossover activity of Sgs1. PLoS Genet 2**:** e155.

Johnson, R., V. Borde, M. J. Neale, A. Bishop-Bailey, M. North *et al.*, 2007 Excess single-stranded DNA inhibits meiotic double-strand break repair. PLoS Genet 3**:** e223.

Joshi, N., A. Barot, C. Jamison and G. V. Börner, 2009 Pch2 links chromosome axis remodeling at future crossover sites and crossover distribution during yeast meiosis. PLoS Genet 5**:** e1000557.

Kane, S. M., and R. Roth, 1974 Carbohydrate metabolism during ascospore development in yeast. J Bacteriol 118**:** 8-14.

Kaur, H., J. S. Ahuja and M. Lichten, 2018 Methods for controlled protein depletion to study protein function during meiosis. Methods Enzymol 601**:** 331-357.

Keeney, S., 2001 Mechanism and control of meiotic recombination initiation. Curr Top Dev Biol 52**:** 1-53.

Keeney, S., C. N. Giroux and N. Kleckner, 1997 Meiosis-specific DNA double-strand breaks are catalyzed by Spo11, a member of a widely conserved protein family. Cell 88**:** 375-384.

Khazanehdari, K. A., and R. H. Borts, 2000 *EXO1* and *MSH4* differentially affect crossing-over and segregation. Chromosoma 109**:** 94-102.

Kirkpatrick, D. T., J. R. Ferguson, T. D. Petes and L. S. Symington, 2000 Decreased meiotic intergenic recombination and increased meiosis I nondisjunction in *exo1* mutants of *Saccharomyces cerevisiae*. Genetics 156**:** 1549-1557.

Lambing, C., K. Osman, K. Nuntasoontorn, A. West, J. D. Higgins *et al.*, 2015 Arabidopsis PCH2 mediates meiotic chromosome remodeling and maturation of crossovers. PLoS Genet 11**:** e1005372.

Lee, S. E., J. K. Moore, A. Holmes, K. Umezu, R. D. Kolodner *et al.*, 1998 *Saccharomyces* Ku70, Mre11/Rad50 and RPA proteins regulate adaptation to G2/M arrest after DNA damage. Cell 94**:** 399-409.

Lichten, M., and J. E. Haber, 1989 Position effects in ectopic and allelic mitotic recombination in *Saccharomyces cerevisiae*. Genetics 123**:** 261-268.

Lynn, A., R. Soucek and G. V. Borner, 2007 ZMM proteins during meiosis: crossover artists at work. Chromosome Res 15**:** 591-605.

Malkova, A., F. Klein, W. Y. Leung and J. E. Haber, 2000 HO endonuclease-induced recombination in yeast meiosis resembles Spo11-induced events. Proc Natl Acad Sci U S A 97**:** 14500-14505.

Mancera, E., R. Bourgon, A. Brozzi, W. Huber and L. M. Steinmetz, 2008 High-resolution mapping of meiotic crossovers and non-crossovers in yeast. Nature 454**:** 479-485.

Manhart, C. M., and E. Alani, 2016 Roles for mismatch repair family proteins in promoting meiotic crossing over. DNA Repair (Amst) 38**:** 84-93.

Martini, E., R. L. Diaz, N. Hunter and S. Keeney, 2006 Crossover homeostasis in yeast meiosis. Cell 126**:** 285-295.

Medhi, D., A. S. Goldman and M. Lichten, 2016 Local chromosome context is a major determinant of crossover pathway biochemistry during budding yeast meiosis. Elife 5.

Mimitou, E. P., S. Yamada and S. Keeney, 2017 A global view of meiotic double-strand break end resection. Science 355**:** 40-45.

Neale, M. J., M. Ramachandran, E. Trelles-Sticken, H. Scherthan and A. S. Goldman, 2002 Wild-type levels of Spo11-induced DSBs are required for normal single-strand resection during meiosis. Mol Cell 9**:** 835-846.

Nishant, K. T., A. J. Plys and E. Alani, 2008 A mutation in the putative *MLH3* endonuclease domain confers a defect in both mismatch repair and meiosis in *Saccharomyces cerevisiae*. Genetics 179**:** 747-755.

Nogami, S., T. Fukuda, Y. Nagai, S. Yabe, M. Sugiura *et al.*, 2002 Homing at an extragenic locus mediated by VDE (PI-SceI) in *Saccharomyces cerevisiae*. Yeast 19**:** 773-782.

Oh, S. D., L. Jessop, J. P. Lao, T. Allers, M. Lichten *et al.*, 2009 Stabilization and electrophoretic analysis of meiotic recombination intermediates in *Saccharomyces cerevisiae*. Methods Mol Biol 557**:** 209-234.

Oke, A., C. M. Anderson, P. Yam and J. C. Fung, 2014 Controlling meiotic recombinational repair - specifying the roles of ZMMs, Sgs1 and Mus81/Mms4 in crossover formation. PLoS Genet 10**:** e1004690.

Pan, J., M. Sasaki, R. Kniewel, H. Murakami, H. G. Blitzblau *et al.*, 2011 A hierarchical combination of factors shapes the genome-wide topography of yeast meiotic recombination initiation. Cell 144**:** 719-731.

Panizza, S., M. A. Mendoza, M. Berlinger, L. Huang, A. Nicolas *et al.*, 2011 Spo11-accessory proteins link double-strand break sites to the chromosome axis in early meiotic recombination. Cell 146**:** 372-383.

Romanienko, P. J., and R. D. Camerini-Otero, 2000 The mouse Spo11 gene is required for meiotic chromosome synapsis. Mol Cell 6**:** 975-987.

Schwacha, A., and N. Kleckner, 1994 Identification of joint molecules that form frequently between homologs but rarely between sister chromatids during yeast meiosis. Cell 76**:** 51-63.

Smagulova, F., I. V. Gregoretti, K. Brick, P. Khil, R. D. Camerini-Otero *et al.*, 2011 Genome-wide analysis reveals novel molecular features of mouse recombination hotspots. Nature 472**:** 375-378.

Subramanian, V. V., A. J. MacQueen, G. Vader, M. Shinohara, A. Sanchez *et al.*, 2016 Chromosome synapsis alleviates Mek1-dependent suppression of meiotic DNA repair. PLoS Biol 14**:** e1002369.

Subramanian, V. V., X. Zhu, T. E. Markowitz, L. A. Vale-Silva, P. San-Segundo *et al.*, 2018 Persistent DNA-break potential near telomeres increases initiation of meiotic recombination on short chromosomes. bioRxiv doi: 10.1101/201889.

Tsubouchi, H., and H. Ogawa, 2000 Exo1 roles for repair of DNA double-strand breaks and meiotic crossing over in *Saccharomyces cerevisiae*. Mol Biol Cell 11**:** 2221-2233.

Wang, T. F., N. Kleckner and N. Hunter, 1999 Functional specificity of MutL homologs in yeast: evidence for three Mlh1-based heterocomplexes with distinct roles during meiosis in recombination and mismatch correction. Proc Natl Acad Sci U S A 96**:** 13914-13919.

Whitby, M. C., 2005 Making crossovers during meiosis. Biochem Soc Trans 33**:** 1451-1455.

Zakharyevich, K., Y. Ma, S. Tang, P. Y. Hwang, S. Boiteux *et al.*, 2010 Temporally and biochemically distinct activities of Exo1 during meiosis: double-strand break resection and resolution of double Holliday junctions. Mol Cell 40**:** 1001-1015.

Zakharyevich, K., S. Tang, Y. Ma and N. Hunter, 2012 Delineation of joint molecule resolution pathways in meiosis identifies a crossover-specific resolvase. Cell 149**:** 334-347.

Zanders, S., and E. Alani, 2009 The *pch2*Δ mutation in baker's yeast alters meiotic crossover levels and confers a defect in crossover interference. PLoS Genet 5**:** e1000571.

Zickler, D., and N. Kleckner, 1999 Meiotic chromosomes: integrating structure and function. Annu Rev Genet 33**:** 603-754.

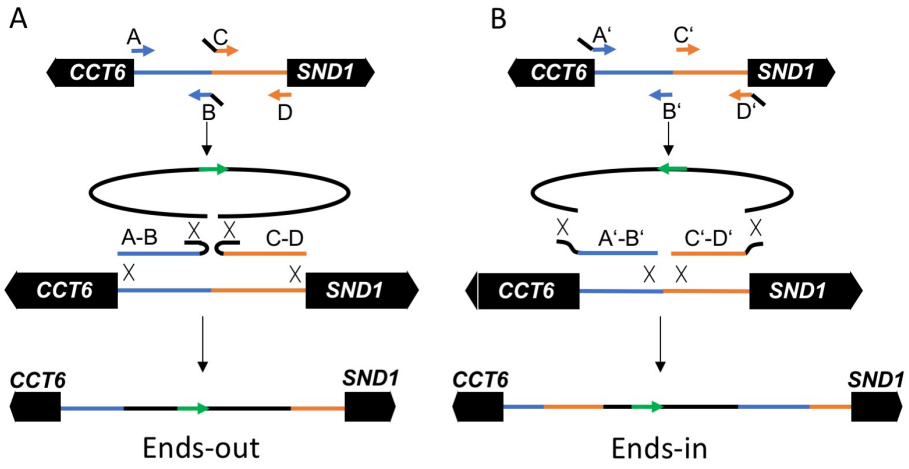

Figure S1. Construction of inserts. Strategy used for insertion in the *CCT6-SND1* intergenic region is illustrated. (At) Ends-out transformation, resulting in an insert that disrupts the intergenic region. PCR products corresponding to the two halves of the region are amplified, using inside primers (B and C) with homology (black lines) to the sequences to be inserted. (B) Ends-in transformation, resulting in a duplication of the intergenic region. PCR products are amplified as above, but with outside primers (A' and D') with homology to sequences to be inserted.

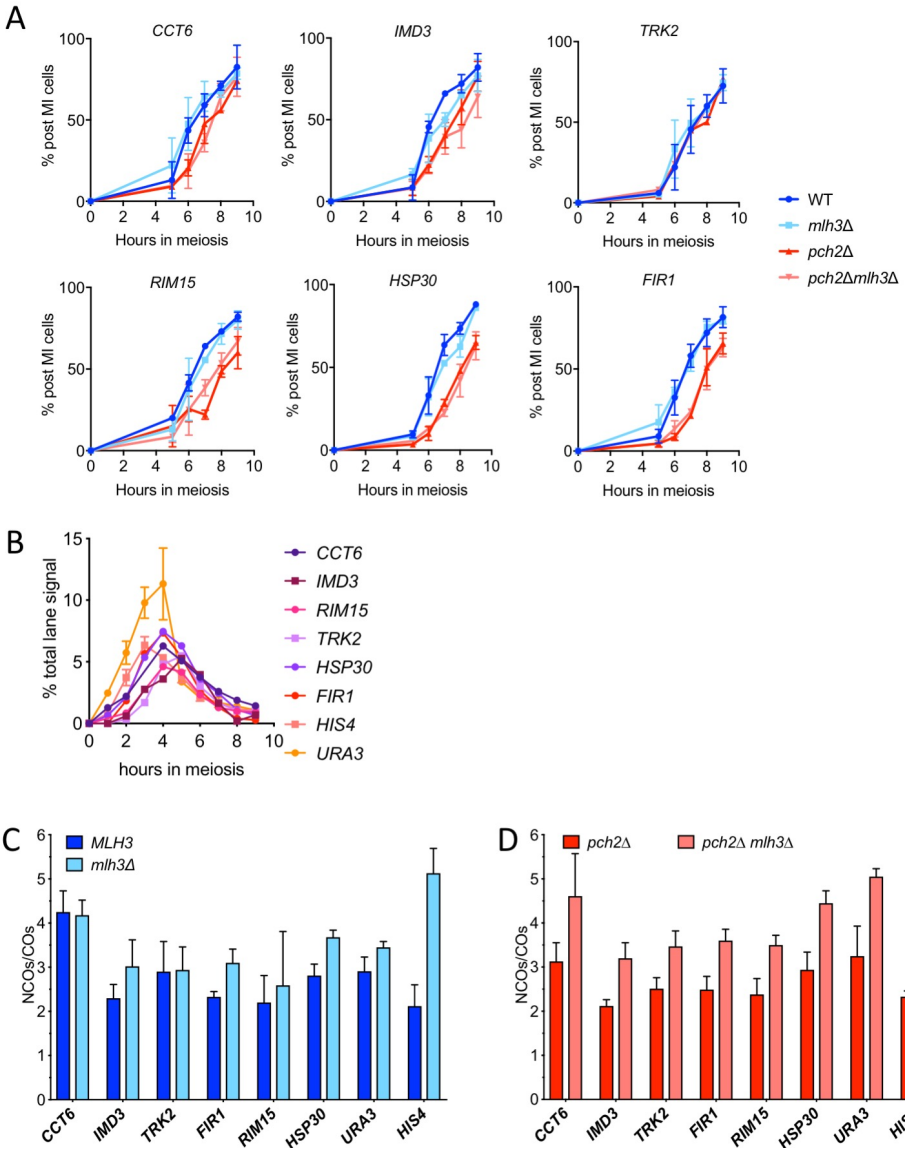

Figure S2: (A) Fraction of cells completing meiosis I, scored in DAPI-stained samples as cells with 2 or more nuclei. (B) VDE-initiated DSBs, scored as percent total lane signal in Southern blots containing *Hin*dIII digests (MEDHI *et al*, 2016). Data for inserts at *HIS4* and *URA3* are from Medhi et al (2016); data for all other insert loci are from a single experiment. (C) NCO/CO ratios for *PCH2* strains, calculated from mean values presented in Figure 3C, D. (D) NCO/CO ratios for *pch2*Δ strains, calculated from mean values presented in Figure 4A, B. For panels (C) and (D), error bars represent the sum of fractional standard deviations for each mean value. In panel (C), NCO/CO ratios in *MLH3* differ significantly from *mlh3*Δ only for inserts at *FIR1*, *HSP30*, and *HIS4* (adjusted p values of 0.02, 0.008 and 0.00001, respectively). In panel (D), NCO/CO ratios in *MLH3 pch2*Δ differ significantly from *mlh3*Δ *pch2*Δ differ significantly for all inserts (adjusted p values all ≤ 0.3).

Table S1: Primers for all reporter inserts

Primers are color-coded to correspond with Figure S1: black—plasmid sequences; tan or blue—corresponding yeast chromosomal sequences.

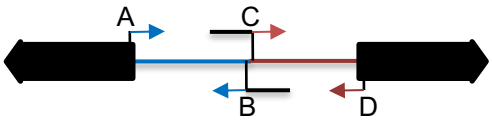

Ends-out transformations

Strain	Primer	sequence
CCT6- SND1	VRS primer A	TGTCTGCTGCATGTTGGAGT
CCT6- SND1	VRS primer B	atcatgcccctgagctgcgcacgtcaagactgtcaaggaagcttgcggccGTTGCCATGCTTACCGTTCT
CCT6- SND1	VRS primer C	tttcacctcttagtcttctggcctcgaggcgagctcgaattcaagcttgcGTTAACGTCGTCGCTTCTCC
CCT6- SND1	VRS primer D	GGATTGTAAGCCCTCAGCAG
IMD3- ATG23	VRS primer A	TATCCTTCCGGATGCTTGTC
IMD3- ATG23	VRS primer B	atcatgcccctgagctgcgcacgtcaagactgtcaaggaagcttgcggccACTGGGTCACTGGAAAAAGG
IMD3- ATG23	VRS primer C	tttcacctcttagtcttctggcctcgaggcgagctcgaattcaagcttgcTTGTGTTCATTTCTAACTCTGGT
IMD3- ATG23	VRS primer D	GTCCATTGGAGAGGAAACGA
RIM15- HAC1	VRS primer A	TAGTGGCGGTTGTTGTCG
RIM15- HAC1	VRS primer B	atcatgcccctgagctgcgcacgtcaagactgtcaaggaagcttgcggccAGAAAAACCTGGAAATATAGTCACG
RIM15- HAC1	VRS primer C	tttcacctcttagtcttctggcctcgaggcgagctcgaattcaagcttgcTTTCCTCGTCCCTTTTGTGG
RIM15- HAC1	VRS primer D	CGGCTGCCTTTATCTTGAAC
TRK2- NAP1	VRS primer A	ACACTTCTGCAGGTCCATCC
TRK2- NAP1	VRS primer B	atcatgcccctgagctgcgcacgtcaagactgtcaaggaagcttgcggccCAAAGTGTCAAGCCGTTGTG
TRK2- NAP1	VRS primer C	tttcacctcttagtcttctggcctcgaggcgagctcgaattcaagcttgcGCATAGCGACGGGATTAGAG
TRK2- NAP1	VRS primer D	CGACAGCGTGATCAGGTAGA
HSP30	VRS primer A	CATCGTCCGTAGCATGGTG
HSP30	VRS primer B	atcatgcccctgagctgcgcacgtcaagactgtcaaggaagcttgcggccCGCTGTTAATTCAAATCGTGGG
HSP30	VRS primer C	tttcacctcttagtcttctggcctcgaggcgagctcgaattcaagcttgcATCCAAGGCGGAAATGTCGTC
HSP30	VRS primer D	GGGCTTAATCCACCACATGGC
FIR1- ZRG8	VRS primer A	GATGAGGATGAAGATGTAGGC
FIR1- ZRG8	VRS primer B	atcatgcccctgagctgcgcacgtcaagactgtcaaggaagcttgcggccCAGAATTGGCATGTCTGAA
FIR1- ZRG8	VRS primer C	tttcacctcttagtcttctggcctcgaggcgagctcgaattcaagcttgcCTACCAAAGATCATCCTTGGCA
FIR1- ZRG8	VRS primer D	CGCATAGTTTTAATGGGAAATTAAC
HSP30	VRS103 primer A	CATCGTCCGTAGCATGGTG
HSP30	VRS103 primer B	aaatcaaaaaaaagaataaaaaaaaaatgatgaattgaattgaagcggccCGCTGTTAATTCAAATCGTGGG
HSP30	VRS103 primer C	tggtatggcttcattcagctccggttcccaacgatcaaggcgaagcttgcATCCAAGGCGGAAATGTCGTC
HSP30	VRS103 primer D	GGGCTTAATCCACCACATGGC
FIR1- ZRG8	VRS103 primer A	GATGAGGATGAAGATGTAGGC
FIR1- ZRG8	VRS103 primer B	aaatcaaaaaaaagaataaaaaaaaaatgatgaattgaattgaagcggccCAGAATTGGCATGTCTGAA
FIR1- ZRG8	VRS103 primer C	tggtatggcttcattcagctccggttcccaacgatcaaggcgaagcttgcCTACCAAAGATCATCCTTGGCA
FIR1- ZRG8	VRS103 primer D	CGCATAGTTTTAATGGGAAATTAAC

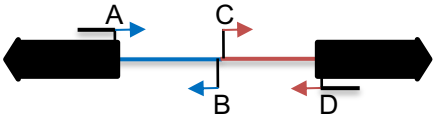

Ends-in transformations

Strain	Primer	sequence
CCT6- SND1	VRS103 primer A	tggtatggcttcattcagctccggttcccaacgatcaaggcgaagcttgcTGTCTGCTGCATGTTGGAGT
CCT6- SND1	VRS103 primer B	GTTGCCATGCTTACCGTTCT
CCT6- SND1	VRS103 primer C	GTTAACGTCGTCGCTTCTCC
CCT6- SND1	VRS103 primer D	aaatcaaaaaaaagaataaaaaaaaaatgatgaattgaattgaagcggccGGATTGTAAGCCCTCAGCAG
IMD3- ATG23	VRS103 primer A	tggtatggcttcattcagctccggttcccaacgatcaaggcgaagcttgcTATCCTTCCGGATGCTTGTC
IMD3- ATG23	VRS103 primer B	TCTTGTTGGATCTCGGAAGG
IMD3- ATG23	VRS103 primer C	GGGACCCTTGGAGGTTTACT
IMD3- ATG23	VRS103 primer D	aaatcaaaaaaaagaataaaaaaaaaatgatgaattgaattgaagcggccGTCCATTGGAGAGGAAACGA
RIM15- HAC1	VRS103 primer A	tggtatggcttcattcagctccggttcccaacgatcaaggcgaagcttgcTAGTGGCGGTTGTTGTCG
RIM15- HAC1	VRS103 primer B	CTTCCAGGAGTGGTTAAGAGG
RIM15- HAC1	VRS103 primer C	GCCTGCTGTAGAGGTTCTG
RIM15- HAC1	VRS103 primer D	aaatcaaaaaaaagaataaaaaaaaaatgatgaattgaattgaagcggccCGGCTGCCTTTATCTTGAAC
TRK2- NAP1	VRS103 primer A	tggtatggcttcattcagctccggttcccaacgatcaaggcgaagcttgcACACTTCTGCAGGTCCATCC
TRK2- NAP1	VRS103 primer B	CAAAGTGTCAAGCCGTTGTG
TRK2- NAP1	VRS103 primer C	GCATAGCGACGGGATTAGAG

Table S2: Strain Genotypes

Strain name	Relevant genotype	Figure
MJL3906, 3907	*CCT6'-natMX-[arg4-VRS]-KlTRP1-'SND1 pCUP1* *CCT6-SND1'-URA3-[arg4-VRS103]-'CCT6-SND1 pCUP1-VDE-hygMX-pCUP1-CUP1*	3, S1
MJL3915	MJL3907 + *mlh3Δ::KanMX/mlh3Δ::KanMX*	3, S1
MJL3944, 3945	MJL3907 + *pch2Δ::URA3/pch2Δ::TRP1*	4, S1
MJL3952, 3953	MJL3907 + *pch2Δ::URA3/pch2Δ::TRP1, mlh3Δ::KanMX/mlh3Δ::KanMX*	4, S1
MJL3908, 3909	*IMD3'-natMX-[arg4-VRS]-KlTRP1-'AGT23 pCUP1* *IMD3-ATG23'-URA3-[arg4-VRS103]-'IMD3-AGT23 pCUP1-VDE-hygMX-pCUP1-CUP1*	3, S1
MJL3916, 3917	MJL3909 + *mlh3Δ::KanMX/mlh3Δ::KanMX*	3, S1
MJL3946, 3947	MJL3909 + *pch2Δ::URA3/pch2Δ::TRP1*	4, S1
MJL3954	MJL3909 + *pch2Δ::URA3/pch2Δ::TRP1, mlh3Δ::KanMX/mlh3Δ::KanMX*	4, S1
MJL3910, 3911	*RIM15'-natMX-[arg4-VRS]-KlTRP1-'HAC1 pCUP1* *RIM15-HAC1'-URA3-[arg4-VRS103]-'RIM15-HAC1 pCUP1-VDE-hygMX-pCUP1-CUP1*	3, S1
MJL3918, 3919	MJL3911 + *mlh3Δ::KanMX/mlh3Δ::KanMX*	3, S1
MJL3948, 3949	MJL3911 + *pch2Δ::URA3/pch2Δ::TRP1*	4, S1
MJL3955, 3956	MJL3911 + *pch2Δ::URA3/pch2Δ::TRP1, mlh3Δ::KanMX/mlh3Δ::KanMX*	4, S1
MJL3912, 3913	*TRK2'-natMX-[arg4-VRS]-KlTRP1-'FMP46 pCUP1* *TRK2-FMP46'- URA3-[arg4-VRS103]-'TRK2-FMP46 pCUP1-VDE-hygMX-pCUP1-CUP1*	3, S1
MJL3920, 3921	MJL3913 + *mlh3Δ::KanMX/mlh3Δ::KanMX*	3, S1
MJL3950, 3951	MJL3913 + *pch2Δ::URA3/pch2Δ::TRP1*	4, S1
MJL3957, 3958	MJL3913 + *pch2Δ::URA3/pch2Δ::TRP1, mlh3Δ::KanMX/mlh3Δ::KanMX*	4, S1
MJL3879	*hsp30::URA3-[arg4-VRS103] pCUP1* *hsp30::natMX-[arg4-VRS]-KlTRP1 pCUP1-VDE-hygMX-pCUP1-CUP1*	3, S1
MJL3881	MJL3879 + *mlh3Δ::KanMX/mlh3Δ::KanMX*	3, S1
MJL3976, 3977	MJL3879 + *pch2Δ::URA3/pch2Δ::TRP1*	4, S1
MJL3970, 3978	MJL3879 + *pch2Δ::URA3/pch2Δ::TRP1, mlh3Δ::KanMX/mlh3Δ::KanMX*	4, S1
MJL3880	*FIR1'-URA3-[arg4-VRS103]-'ZRG8 pCUP1* *FIR1'-natMX-[arg4-VRS]-KlTRP1-'ZRG8 pCUP1-VDE-hygMX-pCUP1-CUP1*	3, S1
MJL3971, 3972	MJL3880 + *mlh3Δ::KanMX/mlh3Δ::KanMX*	3, S1
MJL3969, 3973	MJL3880 + *pch2Δ::URA3/pch2Δ::TRP1*	4, S1
MJL3974, 3975	MJL3880 + *pch2Δ::URA3/pch2Δ::TRP1, mlh3Δ::KanMX/mlh3Δ::KanMX*	4, S1

All strains are homozygous for *lys2*, *ho::LYS2*, *ura3Δ(hindIII-smaI)*, *leu2*, *arg4Δ(eco47III-hpaI)*, *trp1::hisG*, and *VMA1-103*. *pch2Δ::URA3* and *pch2Δ::TRP1* delete sequences between *Acc*I and *Bam*HI and between *Acc*I and *Spe*I sites in *PCH2* coding sequences, respectively. Multiple strain names for a given genotype represent independently derived diploids, both of which were used.